THE ASTROPHYSICAL JOURNAL, 260:488–494, 1982 September 15

THE PECULIAR GALAXY ABELL 76

D. L. TALENT[1]
Yerkes Observatory, University of Chicago
J. B. KALER, J. S. GALLAGHER,[1] AND D. A. HUNTER[1]
Astronomy Department, University of Illinois
Received 1981 December 28; accepted 1982 March 26

ABSTRACT

New spectrophotometric and imaging observations are presented for the peculiar galaxy Abell 76. This is clearly a small but beautiful morphological member of the ring galaxy class. The presence of extensive optical line emission, high surface brightness, and a pronounced blue continuum suggest this object is currently experiencing a very high star formation rate. This event might have been triggered by a collision with another galaxy, which could also account for the ring structure. In addition, spectrophotometric observations reveal a near-solar metallicity in the gas, which is unusual for such a low-luminosity galaxy and provides another indication of an odd evolutionary history.

Subject headings: galaxies: evolution — galaxies: individual — galaxies: structure

I. INTRODUCTION

Abell 76 (PK 50−36°, see Perek and Kohoutek 1967) was described by Abell (1966) as a regular, symmetrical planetary nebula, 13″ in diameter, having the appearance of a ring with gaps. He estimated the apparent photographic and photo-red magnitudes to be $m_{pg} = 15.6$ and $m_{pr} = 14.3$.

That Abell 76 is not a galactic planetary nebula was first pointed out by Chopinet (1971). With the 1.2 m telescope of the Haute-Provence Observatory and an image-tube spectrograph, operating at a dispersion of 420 Å mm^{-1}, she obtained a spectrum that showed several redshifted features (Hα, Hβ, [O III], and [S II]) superposed on an underlying continuum. From the shifts of the emission lines, Chopinet found the radial velocity of Abell 76 to be 3240 ± 40 km s^{-1}. Adopting a value for the Hubble parameter of 100 km s^{-1} Mpc^{-1}, this velocity yielded a distance to Abell 76 of about 32 Mpc and an absolute magnitude of about −17, consistent with a small galaxy. The misclassification of Abell 76 has also been noted in a recent list compiled by Kohoutek (1978).

In her paper, Chopinet (1971) presented only qualitative information on the intensities of the identified emission lines. In this paper, we report on the first quantitative spectrophotometry of Abell 76 and discuss the peculiar nature of this galaxy.

[1]Visiting Astronomer, Kitt Peak National Observatory, which is operated by the Association of Universities for Research in Astronomy, Inc., under contract with the National Science Foundation.

II. OBSERVATIONS

We have observed Abell 76 with a variety of instruments. The pertinent data are summarized in the observing log, Table 1. We obtained three sets of spectra, one with the University of Arizona red Reticon at the 2.3 m telescope of Steward Observatory (SO) and two with the IIDS at Kitt Peak National Observatory (KPNO) 2.1 m. In addition, a video camera image was obtained with the latter telescope. Finally, we used the University of Illinois 1 m telescope at Prairie Observatory (PO) for total wide-aperture narrow-band continuum photometry. Each of the following subsections discusses the acquisition of the data, and the most interesting and obvious features and interpretations.

a) Video Camera

Images of Abell 76 were obtained in R, B, and rest-frame narrow-band Hα filters with the Kitt Peak video camera (Robinson *et al.* 1979) on the 2.1 m telescope. The structure of Abell 76 is very similar in all three colors (Hα emission was redshifted out of our Hα bandpass), and in Figure 1 (Plate 18) we show the R image, which has the best spatial resolution. The contrast of this print was chosen to show the complex structure of the ring, but deeper cuts through the video camera images and an examination of the Palomar Sky Survey (PSS) reveal that the outer edge of the ring remains remarkably sharp even at low brightness levels. Morphologically, Abell 76 is indeed similar to many planetary nebulae.

As an extragalactic system, Abell 76 is clearly an archetypal ring galaxy, most likely of type RK0 in which

TABLE 1

OBSERVING LOG

Telescope	Instrument	Date	λ	Δλ (Å)	Aperture	Position	Integration (s)	Comments
SO 2.3 m	red reticon	1980 Jun 10	4600–7000	12	5″	4″ north	600	
KPNO 2.1 m	IIDS	1981 Jun 3	3550–5350	10	8.″4	center	2400	cirrus
		1981 Jun 4	4730–6850	11	8.″4	center	1200	
KPNO 2.1 m	video camera	1981 Jun 11	$B, R, H\alpha$	...	...	...	...	
PO 1 m	Olson photometer	1980 Jul 16	6593,6566,6503	60,34,33	40″	whole	360	interference filters
		1980 Jul 24	5500,4861	208,17	40″	whole	180	

a "nucleus" is seen projected against the ring (Theys and Spiegel 1976). These rare objects are believed to result from interactions between galaxies, in which a ringlike density enhancement in gas and stars is produced in the disk of one member of a colliding pair (Lynds and Toomre 1976; Theys and Spiegel 1977). However, Abell 76 has no obvious nearby galaxies, and thus if a collision is responsible, then it is either still in progress or one of the systems is optically invisible (cf. Freeman and de Vaucouleurs 1974). In this situation, observations to determine the properties and radial velocity of the embedded "star" (labeled A in Fig. 1), which could well be part of the colliding object, would be of particular interest in further defining the types of collisions that produce R galaxies. Abell 76, however, does stand out from most ring galaxies because of its small size (major axis ~ 2 kpc; most other rings are larger than 8 kpc; $H_0 = 100$ km s^{-1} Mpc^{-1}).

b) *Spectrophotometry*

We obtained spectra of Abell 76 in two positions, at the center and in the ring 4″ north of the center (see Fig. 1). We used the usual beam-switching mode for simultaneous sky subtraction, and processed the data with standard University of Arizona and KPNO reduction programs and the standard atmospheric extinction. The blue and red IIDS spectra of the central region are shown in Figure 2. The galaxy displays a low-excitation emission-line spectrum superposed on a stellar continuum. Figure 2 also shows a number of absorption features, including a distinct Balmer continuum depression. The SO Reticon spectrum of the ring is outwardly similar, showing that the emission-line gas pervades the object.

We present the spectrophotometric results in Tables 2A and 2B. Columns (4) and (5) of Table 2A give relative line fluxes of the center and northern ring, and columns (6) and (7) give these fluxes corrected for interstellar extinction, according to $\log I = \log F + cf_\lambda$. Our f_λ are taken from Torres-Peimbert and Peimbert's (1977) tabulation of the Whitford (1958) function, and the extinction constant, c (row [1] of Table 2B), is derived from the observed $H\alpha/H\beta$ ratio. However, due to the large continuum contribution and probable presence of underlying Balmer absorption, the observed $H\alpha/H\beta$ ratio is an upper limit to the true emission-line ratio, and it is likely that the extinction has been overestimated. In addition to the interstellar extinction, Table 2B presents absolute $H\beta$ and continuum surface brightnesses. S_0 represents the observed surface brightness, and S_{corr} that corrected for the appropriate interstellar extinction. The continuum surface brightness, in rows (4) and (5), was measured at an observed wavelength of 5500 Å. The last column of Table 2B presents estimates of total or integrated $H\beta$ and continuum fluxes, based on the observed surface fluxes. In order to derive the total fluxes we assume that the galaxy can be broken into two components: a uniform disk 4.″2 in radius (the IIDS aperture) with surface brightness S(center), and an annulus of outer radius 6.″5 (the radius of the galaxy) surrounding the disk, with surface brightness S(north).

The errors on these numbers are difficult to assess. Repeated integrations of the SO data indicate that error due to continuum noise is probably somewhat under $\pm 10\%$. The largest source of error in the relative intensities derives from the weakness of $H\beta$. That the systematic error is small is indicated by the good general agreement between the three sets of spectra. The absolute $H\beta$ fluxes from the red and blue IIDS data agree to within 4%.

Note the strong similarity of the central and northern line intensities, especially after correction for extinction. The gas seems to be fairly uniform and excited by the same types of stars. Note also that the stellar contribution at λ5500 is relatively greater in the north than at the center. In spite of the similarity between the two sets of emission lines, the continuum energy distributions of the central and northern regions are quite different. These are shown corrected for extinction in Figures 3 and 4 respectively. The northern continuum is much steeper, indicating a higher percentage of hot stars. Blackbody curves are fitted by least-squares to both sets of data. A 35,000 K curve provides the best fit, although given the possibility of a 7% or 8% systematic error and the difficulties in assigning a proper extinction, 17,000–

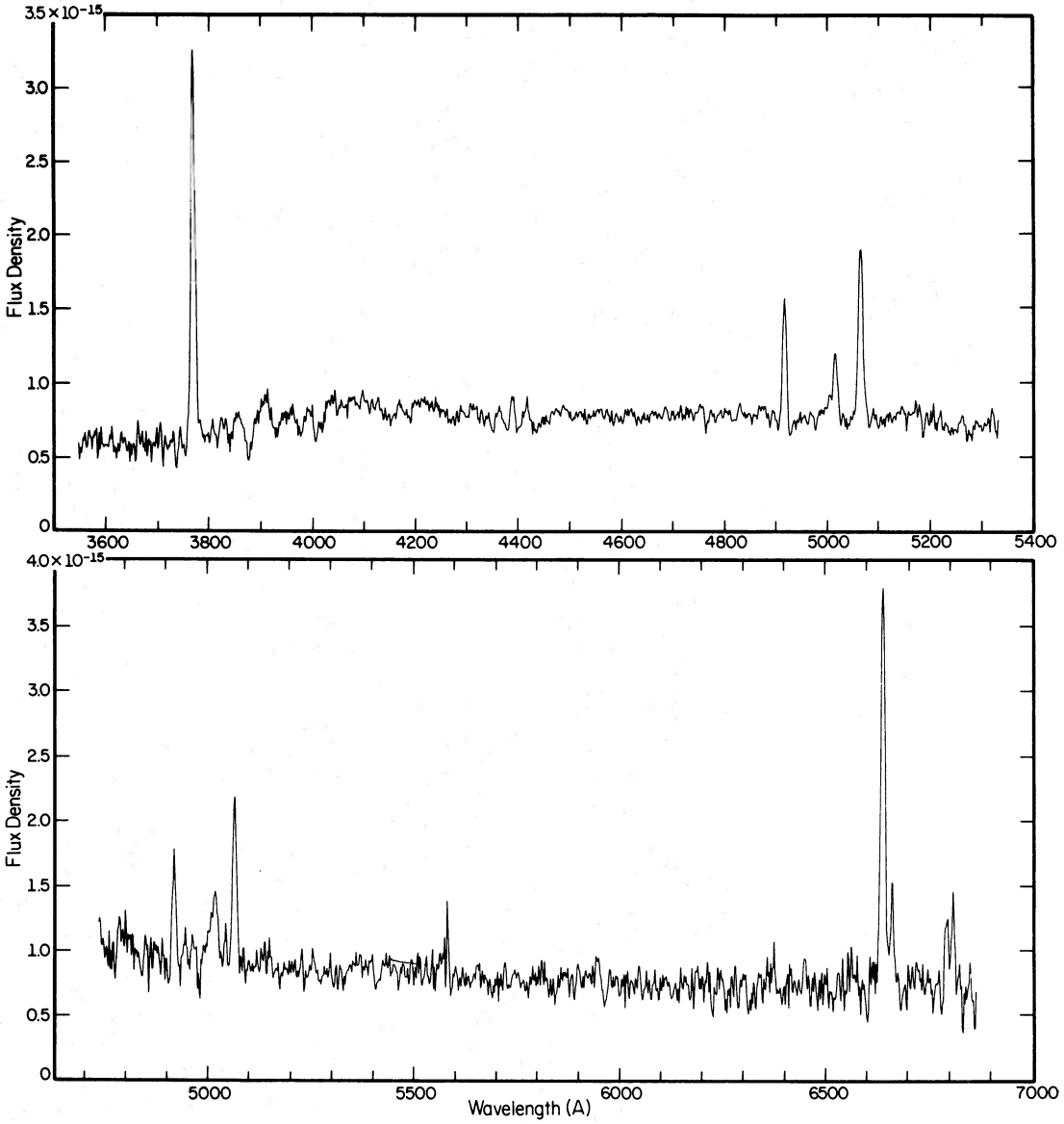

FIG. 2.—Red and blue spectra of the central region of Abell 76; the y-axis is the flux density in ergs cm^{-2} s^{-1} $Å^{-1}$ for the 8″.4 diameter aperture.

20,000 K is certainly acceptable. The central continuum is fitted with 8000 K and 10,000 K curves. Neither of these fit very well because of the obvious deviations from a blackbody for the cooler stars: note especially the clear Balmer discontinuity. The 10,000 K curve fits fairly well longward of 4000 Å, however, and serves to illustrate the average cooler nature of this set of stars. The average spectral type suggested by the absorption lines would be in the neighborhood of F0 to F4, implying an effective temperature somewhat under that of the fitted curves. From $I(\lambda 5007)/I(H\beta)$ and Kaler's (1978) calibration, the mean excitation temperature for the stars that ionize the gas is $\leq 32{,}000$ K, similar to the best-fit blackbody for the northern continuum. The types of stars that excite the gas seem similar throughout the galaxy, but there are relatively more of them near the periphery.

c) *Radial Velocities*

We have measured the radial velocity of the galaxy from both the emission and absorption lines; these, and the means, are listed in Table 3. The measured wavelengths for the red IIDS data have been adjusted down-

TABLE 2

PHOTOMETRY OF ABELL 76

A. Observed and Corrected Relative Line Intensities

λ (1)	ID (2)	f_λ (3)	F_{center} (4)	F_{North} (5)	I_{center} (6)	I_{North} (7)	Mean (8)
3727 ...	[O II]	0.315	376	...	556	...	556
4861 ...	Hβ	0.000	100	100	100	100	100
4959 ...	[O III]	−0.020	56	...	55	...	55
5007 ...	[O III]	−0.030	169	187	163	178	170
6563 ...	Hα	−0.335	432	512	286	286	286
6584 ...	[N II]	−0.340	94	119	62	66	64
6717 ...	[S II]	−0.370	74	89	47	47	47
6731 ...	[S II]	−0.370	84	100	53	53	53

B. Extinction and Absolute Photometry

Parameter	Center	North	Total[a]
Hβ extinction, c	0.54	0.75	...
10^{16} S_0(Hβ) ergs cm^{-2} s^{-1} arcsec^{-2}	1.52	1.32	187
10^{16} S_{corr}(Hβ)	5.27	7.42	870
10^{17} $S_0(\lambda 5500)\,d\lambda$ ergs cm^{-2} s^{-1} Å^{-1} arcsec^{-2}	1.38	1.87	222
10^{17} $S_{corr}(\lambda 5500)\,d\lambda$	3.92	8.25	859

NOTE.—V (measured total) = 15.0 ± 0.25.

[a]Total flux = 55 × central surface brightness + 78 × northern surface brightness; see § II*b*.

ward by 0.6 Å (≈30 km s^{-1}) suggested by a slight redward shift of the [O I] night-sky feature from the rest wavelength of λ5577.4. The radial velocities from the northern SO data could not be properly calibrated and serve as confirmation only.

The radial velocity determined from the reliable KPNO data and the measurements of 10 separate emission lines (13 measurements due to overlap of coverage) is 3412 ± 57 (2 σ) km s^{-1}. Each line was given equal weight. Correcting the average for solar motion after the fashion described in the (de Vaucouleurs, de Vaucouleurs, and Corwin (1976), RC2) yields 3600 ± 57 (2 σ) km s^{-1}. The five blue absorption lines exhibit an average radial velocity that is 97 km s^{-1} smaller than

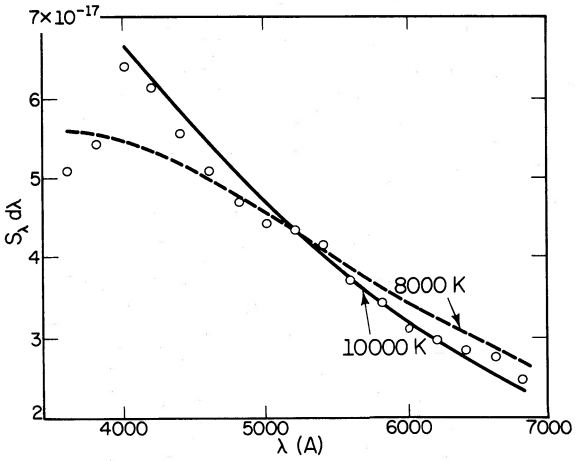

FIG. 3

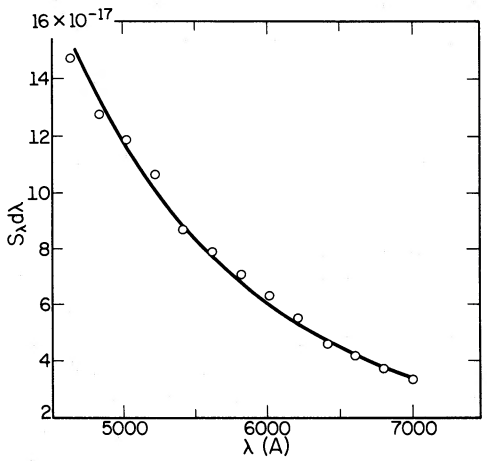

FIG. 4

FIG. 3.—The central continuum surface brightness distribution of Abell 76 in ergs cm^{-2} s^{-1} Å^{-1} arcsec^{-2} corrected for interstellar extinction. *Solid line*, 10,000 K blackbody; *dashed line*, 8000 K blackbody; both shifted appropriate to the observed radial velocity.

FIG. 4.—The northern continuum surface brightness distribution of Abell 76 in ergs cm^{-2} s^{-1} Å^{-1} arcsec^{-1}, corrected for interstellar extinction. The line represents an appropriately shifted 35,000 K blackbody.

TABLE 3

RADIAL VELOCITY OF ABELL 76

A. Emission Lines

λ_0	V (center) km s^{-1} IIDS-Jun 3	V_r (center) km s^{-1} IIDS-Jun 4	V_r (north)[a] km s^{-1}
3727.5 ...	3410	...	...
3868.8 ...	3379	...	...
4340.5 ...	3378	...	...
4861.3 ...	3429	3416	3024
4958.9 ...	3410	3440	...
5006.8 ...	3443	3401	3176
6562.8 ...	...	3408	3108
6583.4 ...	...	3474	3190
6716.4 ...	...	3366	3171
6730.8 ...	...	3403	3209
Mean[b] ...	3408±48	3415±63	3146±28

B. Absorption Lines

λ_0	V (center) km s^{-1} IIDS-Jun 3
3797.9 ...	3402
3835.4 ...	3267
3889.1 ...	3299
3933.7 ...	3361
3968.5 ...	3248
Mean	3315±116

[a]Not calibrated, confirmation only

[b]Mean, all emission lines = 3412±57 km s^{-1}; corrected for solar motion = 3600±57 km s^{-1}; Chopinet 1971 = 3240 ±40 km s^{-1}.

the emission-line average, 3315±116 (2 σ) km s^{-1}. The difference is only marginally significant. The values presented here agree favorably with Chopinet's (1971) value of 3240 km s^{-1}.

d) *Magnitude*

The total continuum flux density of Abell 76 was observed with the PO 1 m telescope and several interference filters centered in line-free spectral regions (see Table 1). Because the errors on the individual observations were fairly high, and because of clear systematic differences between the two nights, we calculated the V-magnitude by scaling all the data to λ5500, where we used the mean of the continuous energy distributions in Figures 3 and 4. The mean result for all filters is $V = 15.0 \pm 0.25$, which is entered as a note to Table 2B. Equivalent V-magnitudes from the individual filters range from 14.7±0.1 (internal error) for the mean of the red set to 15.55±0.35 for the single λ5500 observation.

An estimate of the V-magnitude can also be made from the total λ5500 continuum surface flux listed in the last column of Table 2B (see § II*b*). The result is $V = 15.5$. The difference between the two measures is probably due to the additional object (the "nucleus") seen in Figure 1 that was included in the PO data but not in the surface brightness observations. The fainter value might be more appropriate for Abell 76 proper, sans "companion." The "companion" would then be very roughly of magnitude 16.1.

The apparent magnitude of $V = 15.0$ implies an absolute magnitude of $M_V = -17.8$ for $H = 100$ (see Table 5). This indicates that Abell 76 deviates very strongly from the normal relationship between absolute magnitude and linear diameter for galaxies (Holmberg 1975) in the sense that it has much higher than usual surface brightness. It seems likely that this anomaly could also be associated with the system's structural peculiarities, e.g., an epoch of enhanced star formation may have been triggered by a collision (Larson and Tinsley 1978).

III. CHEMICAL ABUNDANCES

The data of Table 2 allow a crude estimate of the mean chemical composition of the interstellar gas in Abell 76. The limiting factors are: (1) that we have not observed a temperature-sensitive line such as λ4363 [O III] or λ5754 [N II], and (2) underlying H-Balmer absorption may have effected the strengths of hydrogen emission lines. A comparison of the [O II] and [O III] intensities with the figures presented by Pagel *et al.* (1979) suggests a nominal oxygen abundance of 2.4×10^{-4} and a nebular temperature of about 9600 K.

We find the mean electron density from the [S II] λ6731/λ6717 ratio, using Saraph and Seaton's (1970) emission coefficients updated by the more recent calculations of Pradhan (1978), to be $N_e \approx 2 \times 10^3$ cm^{-3}. This high value of N_e suggests that the emission lines are not coming from a general diffuse interstellar gas but are produced by a large number of discrete H II regions.

We have computed abundance ratios based upon this density for both $T_e = 9600$ K and for comparison, 12,000 K, where the parameters used are essentially those of Osterbrock (1974) except for S^+ and O^+, where new collision strengths from Pradhan (1978, 1976) were used respectively. The results are shown in Table 4. Given the

TABLE 4

CHEMICAL COMPOSITION OF ABELL 76

Ratio	Abundances $T_e = 9600$[a]	Abundances $T_e = 12000$[a]
O^+/H^+	3.36×10^{-4}	1.31×10^{-4}
O^{2+}/H^+ ...	6.48×10^{-5}	3.19×10^{-5}
N^+/H^+	1.40×10^{-5}	0.79×10^{-5}
S^+/H^+	1.38×10^{-6}	0.77×10^{-6}
O/H	4.01×10^{-4}	1.63×10^{-4}
N/O	0.042	0.061

[a]$N_e \approx 2 \times 10^3$ cm^{-3} from [S II].

TABLE 5

PARAMETERS FOR ABELL 76

H (km s^{-1} Mpc)	D (Mpc)	d (kpc)	$L(\mathrm{H}\beta)$ ($\times 10^{40}$ ergs s^{-1})	$\log_{10}[L(\mathrm{H}\beta)]$	M_V[a]	M_{H}[b] ($\times 10^7 M_\odot$)	$\log_{10}(M_{\mathrm{H}})$
100.....	36	2.27	1.37	40.13	−17.8	1.46	7.16
75.....	48	3.03	2.39	40.38	−18.4	2.60	7.41
50.....	72	4.54	5.39	40.73	−19.3	5.85	7.77

[a] Calculated assuming $V = 15.0$ as per Table 2B.

[b] Calculated using: $M_{\mathrm{H}} = [4D^2 S_{\mathrm{corr}}(\mathrm{H}\beta) m_{\mathrm{H}}]/[(\varepsilon N_e)\alpha(\mathrm{H}\beta)E(\mathrm{H}\beta)]$. For the values of M_H shown in the table it has been assumed that $(\varepsilon N_e) = 6$. If this uncertain quantity were to be increased (decreased) by a factor of 10, the derived value of M_{H} would decrease (increase) by a factor of 10.

latitude in T_e, there is nothing extraordinary about the ratios. The O/H ratio appears low to normal, and the N/O ratio is under 40% of solar, similar to that found for a variety of extragalactic situations.

IV. DISCUSSION

In Table 5 we list the quantities H, D (distance to Abell 76 in Mpc), d (diameter of Abell 76 in kpc), $L(\mathrm{H}\beta)$ (the intrinsic total luminosity in Hβ derived from the total $F(\mathrm{H}\beta)$ of Table 2), $\log_{10}[L(\mathrm{H}\beta)]$, M_V, M_H (mass of ionized hydrogen, in solar masses calculated as per the notes to Table 5), and $\log_{10}(M_H)$. We will choose the case of $H \approx 100$ km s^{-1} Mpc^{-1} for consideration in the following discussion.

An interesting object for comparison to Abell 76 is the H II complex in NGC 2366 (Kennicutt, Balick, and Heckman 1980). The intrinsic Hα luminosity of this object is on the order of 10^{40} ergs s^{-1} (requiring a UV input of about 10^{52} photons s^{-1}), comparable with Abell 76. Kennicutt *et al.* estimate that the required UV input could be provided by 100 O4 stars, 1000 O6 stars, or 10,000 O9 stars. We roughly estimate a required UV input of about 3×10^{52} photons s^{-1} to account for the Abell 76 emission; this could be provided by about 350 O4 stars, 2500 O6 stars, 25,000 O9 stars, or 130,000 B0 stars (see Table 2 of Panagia 1973). This is consistent with the dominance of hot stars found from the continuum energy distribution of Abell 76. Kennicutt *et al.* estimate the mass of the NGC 2366 H II complex as about 10^5–10^6 solar masses; we estimate about 10^7 solar masses of ionized hydrogen for Abell 76, under the assumptions given in the notes to Table 5. We should like to point out that the NGC 2366 H II complex is of much higher excitation than Abell 76, and the oxygen temperature in NGC 2366 region is quite high, in agreement with its rather low oxygen abundance.

From Table 5, for the case being examined, we can see that Abell 76 has an apparent linear diameter on the order of the Small Magellanic Cloud with a luminosity on the order of the Large Magellanic Cloud. Thus, it might prove worthwhile to compare Abell 76 with the "high-luminosity" cases presented by French (1980) in his study of galaxies similar to H II regions. These particular galaxies are characterized by an O/H ratio of about 2.5×10^{-4}, which is similar to the $\sim 2.4 \times 10^{-4}$ value determined for Abell 76. French notes that his "high-luminosity" cases are typically a factor of 2 larger in the O/H ratio quantity than his "low-luminosity" cases and that the galaxies in his sample that fall in the former category are, in all cases, apparently interacting with a companion. Hence, these galaxies are probably not truly "young galaxies" undergoing a "flash" of star formation as French concluded the "low-luminosity" cases most likely are. In a similar fashion, it would seem that Abell 76 is a small galaxy undergoing a particularly vigorous phase of star formation, that might reasonably have been stimulated by the same event that produced the ring morphology. In that the O/H ratio for Abell 76 could be as large as 4×10^{-4}, indicating a near-solar metallicity, it is unlikely that the observed abundances are due to the present burst of star formation activity alone. The physical dimensions, luminosity, morphology, and abundance characteristics, considered together, suggest a rather odd evolutionary history for Abell 76.

This research was supported by NSF grants AST 78-23647 and AST 80-23233 (J. B. K.) and by AST 79-09977 (J. S. G. and D. A. H.) to the University of Illinois. D. L. T. would like to acknowledge support for this research from the Wm. Gaertner Astronomy Fund, University of Chicago. We would also like to thank the staffs of the Kitt Peak National Observatory and Steward Observatory for their help and support.

REFERENCES

Abell, G. O. 1966, *Ap. J.*, **144**, 259.
Chopinet, M. 1971, *C.R. Acad. Sci., Paris*, **272**, 290.
de Vaucouleurs, G., de Vaucouleurs, A., and Corwin, G. H., Jr. 1976, *Second Reference Catalogue of Bright Galaxies* (Austin: University of Texas) (RC2).
Freeman, K. C., and de Vaucouleurs, G. 1974, *Ap. J.*, **194**, 569.
French, H. 1980, *Ap. J.*, **240**, 41.
Holmberg, E. 1975, in *Galaxies and the Universe*, ed. A. Sandage, M. Sandage, and J. Kirstian (Chicago: University of Chicago Press), p. 123.

Kaler, J. B. 1978, *Ap. J.*, **220**, 887.
Kennicutt, R., Balick, B., and Heckman, T. 1980, *Pub. A.S.P.*, **92**, 134.
Kohoutek, L. 1978, in *IAU Symposium 76, Planetary Nebulae Observations and Theory*, ed. Y. Terzian (Dordrecht: Reidel), p. 47.
Larson, R. B., and Tinsley, B. M. 1978, *Ap. J.*, **219**, 46.
Lynds, R., and Toomre, A. 1976, *Ap. J.*, **209**, 382.
Osterbrock, D. 1974, *Astrophysics of Gaseous Nebulae*, (San Francisco: Freeman).
Pagel, B. E. J., Edmunds, M. G., Blackwell, D. E., Chun, M. S., and Smith, G. 1979, *M.N.R.A.S.*, **189**, 95.
Panagia, N. 1973, *A.J.*, **78**, 929.
Perek, L., and Kohoutek, L. 1967, *Catalog of Galactic Planetary Nebulae*, (Prague: Czechoslovakian Academy of Sciences).
Pradhan, A. K. 1976, *M.N.R.A.S.*, **177**, 31.
_____. 1978, *M.N.R.A.S.*, **184**, 89P.
Robinson, W., Bali, W., Vakoy, P., Piegersch, W., and Reed, R. 1979, *SPIE, Instrumentation in Astronomy III*, **172**, 98.
Saraph, H. E., and Seaton, M. J. 1970, *M.N.R.A.S.*, **148**, 367.
Torres-Peimbert, S., and Peimbert, M. 1977, *Rev. Mexicana Astr. Ap.*, **2**, 181.
Theys, J. C., and Spiegel, E. A. 1976, *Ap. J.*, **208**, 650.
_____. 1977, *Ap. J.*, **212**, 616.
Whitford, A. E. 1958, *A.J.*, **63**, 201.

J. S. GALLAGHER: Department of Astronomy, University of Illinois, Urbana, IL 61801

D. A. HUNTER: Department of Astronomy, University of Illinois, Urbana, IL 61801

J. B. KALER: Department of Astronomy, University of Illinois, Urbana, IL 61801

D. L. TALENT: Yerkes Observatory, Williams Bay, WI 53191

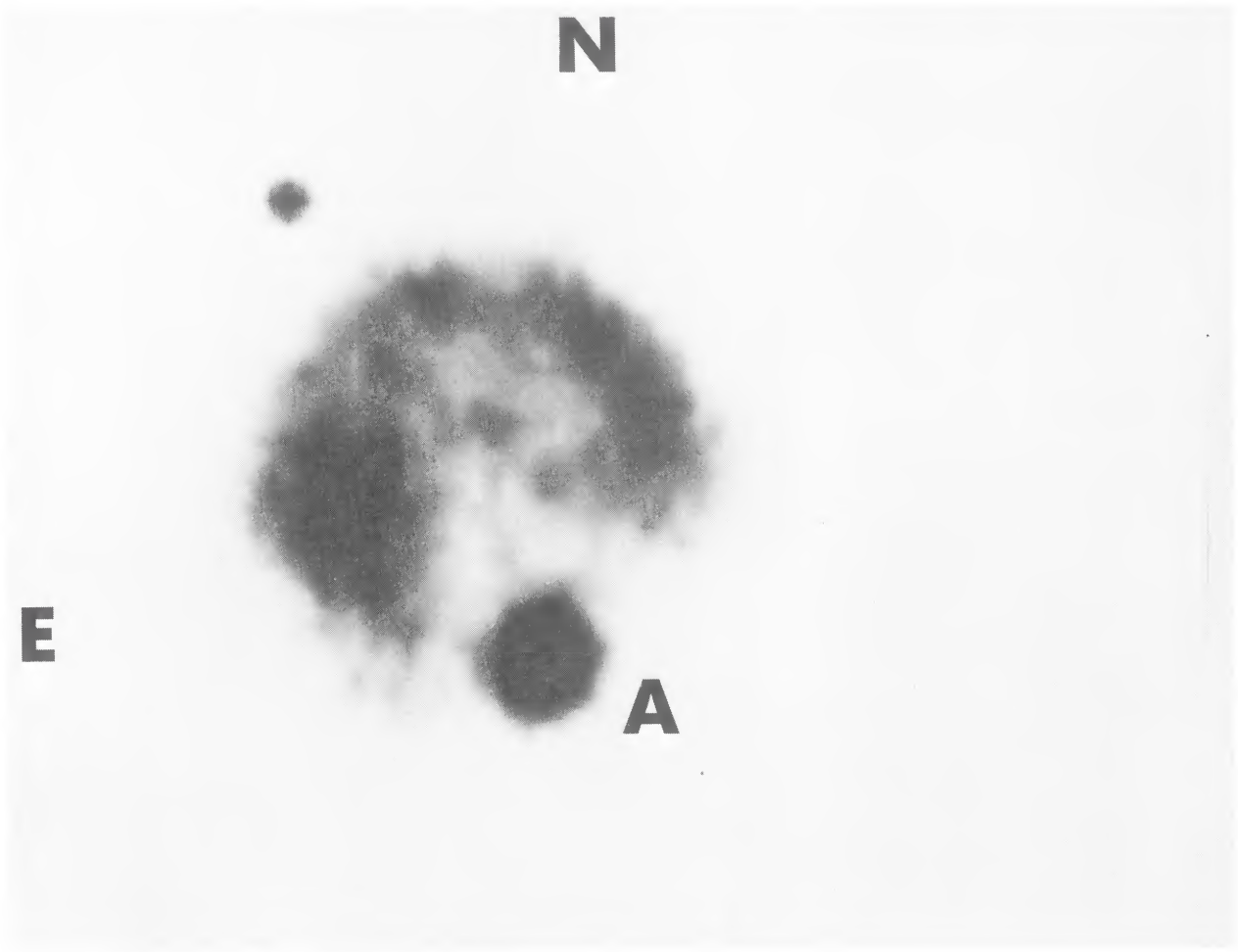

FIG. 1.—Video camera image of Abell 76 through an *R* filter; field of view is 40″ square

TALENT *et al.* (*see* page 488)